Journal of Renewable Materials

Tech Science Press

https://doi.org/10.32604/jrm.2026.02025-0187

ARTICLE

Characteristics of Cellulose from Oil Palm Trunks at Different Ages for Renewable Materials Applications

Elina Hishamuddin*, Fatiha Ismail, Stasha Eleanor Rosland Abel, Humaira Alias Aisyah and Abdul Wahab Noorshamsiana

Biomass Technology Unit, Engineering & Processing Research Division, Malaysian Palm Oil Board, No. 6, Persiaran Institusi, Bandar Baru Bangi, Kajang, Selangor, Malaysia

*Corresponding Author: Elina Hishamuddin. Email: elina@mpob.gov.my

Received: 03 October 2025; Accepted: 04 March 2026; Published: 29 June 2026

ABSTRACT: Oil palm trunks (OPT), abundantly available during plantation replanting, represent a renewable lignocellulosic resource for sustainable material applications. Although OPT-derived cellulose has been extensively explored, the influence of oil palm age on cellulose properties remains insufficiently understood. In this study, cellulose was isolated from OPT aged 21, 25, and 32 years and characterized by scanning electron microscopy (SEM), Fourier-transform infrared spectroscopy (FTIR), X-ray diffraction (XRD), and thermogravimetric analysis (TGA). SEM observations indicated more uniform and better-separated fibril structures in cellulose from older OPT, suggesting more effective removal of non-cellulosic components. FTIR confirmed successful cellulose isolation across all age groups. XRD analysis revealed an increase in crystallinity with trunk age, from 62.94% to 68.62%, while TGA showed slightly enhanced thermal stability for cellulose obtained from older trunks. These age-dependent variations suggest that cellulose from younger OPT is more suitable for chemical modification, whereas cellulose from older OPT is better suited for applications requiring higher structural and thermal stability, such as biocomposites and reinforcement materials. These findings highlight OPT as a valuable renewable feedstock, with its valorization supporting circular bioeconomy strategies through the production of advanced renewable materials.

KEYWORDS: Oil palm trunk; cellulose characterization; crystallinity index; thermal stability; renewable materials

1 Introduction

The global shift towards sustainable and renewable resources has intensified interest in lignocellulosic biomass as a viable alternative for producing eco-friendly materials. Among various agricultural residues, oil palm (*Elaeis guineensis*) biomass stands out due to its abundance, especially in countries like Malaysia and Indonesia, which are leading producers of palm oil. The oil palm trunk (OPT), a major byproduct generated during the replanting process that usually occurs after 25 years of cultivation, represents a substantial source of lignocellulosic material [1].

OPT is primarily composed of cellulose (38%–41%), hemicellulose (12%–17%), and lignin (18%–23%) [2]. The cellulose content of OPT is comparable to that of conventional wood; however, OPT cell walls are generally thinner and contain less lignin, which facilitates fibrillation and makes them more suitable for nanocellulose production. Cellulose, the most abundant component, is a linear polysaccharide consisting of β-1,4-linked D-glucose units. Its unique properties, such as biodegradability, high tensile strength, and renewability, make it an attractive candidate for various applications, including the development of

biocomposites, films, packaging, and other renewable materials [3–5]. The extraction and characterization of cellulose from OPT not only add value to this agricultural waste but also contribute to environmental sustainability by reducing biomass disposal issues and supporting resource-efficient utilization.

Several studies have characterized cellulose derived from OPT and other oil palm biomass, highlighting their potential as renewable material sources. Research indicates that the crystallinity index (CrI) of oil palm biomass cellulose varies significantly depending on the source and processing intensity. For instance, cellulose nanocrystals (CNCs) isolated from oil palm trunks (OPT) have been reported to reach a CrI of 68%–70% [6], while microcrystalline cellulose (MCC) typically ranges between 64% and 78% depending on the extraction method and fiber pretreatment [7]. In comparison, cellulose derived from empty fruit bunches (EFB) often exhibits lower crystallinity, ranging from 54% to 66% due to its higher amorphous content [8], whereas oil palm fronds (OPF) CrI can reach up to 70% [9]. Among the various oil palm components, cellulose nanofibers (CNFs) from OPT demonstrated the highest crystallinity, reaching up to 77%, along with superior mechanical strength [10]. These values are highly competitive with commercial benchmarks; for example, Park et al. (2010) [11] reported that the CrI of commercial celluloses measured by the Segal peak height method ranged from 78.0% to 95.2%, while also noting that CrI values vary significantly depending on the measurement technique used. These studies demonstrate the versatility of oil palm biomass as a cellulose source, with OPT offering advantages in structural integrity and crystallinity relative to OPF and EFB.

Although numerous studies have confirmed the potential of oil palm biomass as a source of cellulose, the influence of replanting age on the characteristics of cellulose extracted from OPT has received limited attention. Trunk age is expected to play a decisive role in determining the chemical composition, fibril arrangement, and lignin content of OPT, which in turn affect key properties such as crystallinity, thermal stability, and fibrillation potential. Most existing work has focused on comparing different oil palm residues or optimizing extraction methods, without considering age-related variations as a determining factor. Understanding these variations is essential, as they directly influence the suitability of the derived cellulose for targeted renewable applications. Addressing this gap provides a pathway to optimize the valorization of OPT across different replanting cycles, thereby advancing its use as a sustainable feedstock for renewable materials.

In this study, we aimed to investigate the characteristics of cellulose extracted from oil palm trunks at different ages. The cellulose content was determined using TAPPI standard methods and cellulose samples were analyzed for their crystallinity using X-ray diffraction (XRD), thermal stability through thermogravimetric analysis (TGA), functional groups via Fourier-transform infrared spectroscopy (FTIR) and scanning electron microscopy (SEM) was employed to observe the morphological features. By correlating these properties with the trunk age, this research seeks to identify the optimal age for harvesting OPT to obtain cellulose with desirable properties for renewable material applications.

2 Materials and Methods

2.1 Materials

The chemicals used in the OPT sample preparation and cellulose extraction process included ethanol (>99.7% purity), toluene (>99.5% purity), sodium chlorite (~80% purity) and sodium hydroxide (>99.0% purity) (R&M Chemicals, Malaysia), and acetic acid (>99.5% purity) and acetone (>99.5% purity) (Systerm, Malaysia). Commercial cellulose (cotton linters) was purchased from Sigma-Aldrich (Malaysia).

2.2 Oil Palm Fibers Preparation

The OPT from the *Elaeis guineensis* Jacq. Tenera (D×P) oil palm species, at 21, 25 and 32 years, were sourced from the MPOB Research Station plantation in Hulu Paka, Terengganu, Malaysia (Fig. 1a). For each age group, OPT samples were collected as composite samples, representing the entire trunk, to ensure uniformity and representativeness of the fibers. The samples were prepared in accordance with the Technical Association of the Pulp and Paper Industry (TAPPI) Test Method T257 cm-22 [12], which provides guidelines for the sampling and preparation of wood for analysis. The OPT fibers (Fig. 1b) were first oven-dried at 105°C for 24 h and weighed repeatedly until a constant weight was achieved. Extractive-free fibers were then obtained by Soxhlet extraction for 6–8 h using an ethanol-toluene mixture (1:2 v/v), and were subsequently used for holocellulose preparation.

(a) (b) (c)

Figure 1: Images of (**a**) OPT logs collected after felling, (**b**) OPT fibers and (**c**) extracted OPT cellulose.

2.3 Cellulose Extraction Method

Prior to cellulose extraction, holocellulose was prepared from the extractive-free fibers following the method of Wise et al. [13] with slight modifications. Approximately 4 g of oven-dried OPT sample was suspended in 200 mL of distilled water in a 250 mL conical flask. Initially, 3 g of sodium chlorite ($NaClO_2$) and 10 mL of 10% (v/v) acetic acid were added, and the mixture was stirred and heated in a boiling water bath for 30 min. Thereafter, fresh portions of 3 g $NaClO_2$ and 10 mL of 10% acetic acid were added at 30 min intervals, until a total of 12 g $NaClO_2$ and 40 mL of acetic acid had been introduced over 1.5 h, followed by a final 30 min heating to complete delignification. The resulting white holocellulose was filtered, washed with distilled water until odorless, rinsed with acetone, and oven-dried at 60°C until a constant weight was achieved.

Cellulose was subsequently isolated from holocellulose following TAPPI Test Method T203 cm-22 [14], which quantifies the alpha-, beta- and gamma-cellulose content in pulp. Approximately 1.5 g of the holocellulose sample was treated with 17.5% NaOH for three 15-min intervals, followed by dilution with distilled water and a 30-min settling period. The residue was then washed with 8.3% NaOH, distilled water, 2N acetic acid, and again with distilled water. The purified cellulose was oven-dried at 105°C to constant weight and the yield was recorded. The cellulose yield (%) was calculated as the ratio of the oven-dried mass of extracted cellulose to the initial oven-dried mass of holocellulose, multiplied by 100. The extracted OPT cellulose (Fig. 1c) from all age groups was subsequently characterized in terms of its morphological, crystalline, thermal, and chemical properties, with the aim of assessing its potential as a renewable material for various applications.

2.4 Morphology Analysis by Scanning Electron Microscope (SEM)

The surface morphology of the extracted OPT fibers and cellulose samples were examined using a scanning electron microscope (SEM) (Hitachi S-2700, USA), at magnifications of 40× and 500×, respectively.

2.5 Fourier Transform Infrared (FTIR) Spectroscopy Analysis

The functional groups and chemical structure of the OPT cellulose samples and commercial cellulose were identified using FTIR spectroscopy. Approximately 3 mg of each sample was used for the analysis. The infrared spectra were recorded with an FTIR spectrometer (PerkinElmer Frontier, USA) over a scanning wavelength range of 650–4000 cm^{-1}, with a resolution of 8 cm^{-1}.

2.6 X-Ray Diffraction (XRD) Analysis

The crystallinity of the OPT cellulose samples and commercial cellulose was evaluated using XRD analysis. Measurements were performed using a Bruker D8 Advance diffractometer (Bruker AXS GmbH, Germany) to characterise the structural ordering of the extracted cellulose samples. Diffraction intensity patterns were recorded over a 2θ range of 5° to 80°, with a scan speed of 7.5°/min and a step size of 0.025°, under operating conditions of 40 kV and 40 mA. Due to the observed shifts in peak positions in the OPT diffractograms, the crystallinity index (CrI) was calculated using a modified application of the Segal method, as shown in Eq. (1) [15].

$$\boldsymbol{CrystallinityIndex, CrI(\%)} = \frac{\boldsymbol{I_{002} - I_{am}}}{\boldsymbol{I_{002}}} \times \mathbf{100\%} \quad (1)$$

where I_{002} was taken as the maximum intensity of the principal diffraction peak in the 20°–23° region for each OPT sample, and I_{am} was determined at the local minimum specific to each OPT diffractogram, which varied depending on the degree of structural disorder.

2.7 Thermogravimetric Analysis (TGA)

The thermal stability of the extracted cellulose from each OPT age and commercial cellulose was evaluated using a thermogravimetric analyzer (PerkinElmer Series Pyris 6 TGA, USA). Approximately 5 mg of each sample was weighed and heated from 30°C to 600°C at a rate of 20°C min^{-1} under a nitrogen atmosphere. Thermogravimetric and derivative thermogravimetric (DTG) curves were analyzed using the Pyris 6 TGA software to assess the thermal stability of the OPT celluloses at different ages and further comparison was made with commercial cellulose.

3 Results and Discussion

3.1 Surface Morphological Analysis

Fig. 2 presents representative SEM micrographs of raw OPT fibers (a–c) and the corresponding extracted cellulose (d–f) from OPT aged 21, 25, and 32 years. It can be seen that the raw OPT fibers (Fig. 2a–c) exhibited dense, compact structures with surface irregularities and deposits, which can be attributed to the presence of non-cellulosic components such as lignin, hemicellulose, and extractives. The fiber sample from 25-year-old OPT (Fig. 2b) displayed a rougher, more layered morphology compared to the 21-year-old sample (Fig. 2a), suggesting progressive accumulation of matrix components with trunk maturity. In comparison, the OPT fibers from the 32-year-old trunk (Fig. 2c) exhibited an even more compact and consolidated surface with pronounced deposits and reduced visible porosity relative to the 21- and 25-year-old samples (Fig. 2a,b), indicative of increased lignification and structural densification with advanced trunk age. These observations

are consistent with earlier reports that describe the complex morphology of lignocellulosic biomass, where the cell walls are reinforced by a matrix of lignin and hemicellulose [16].

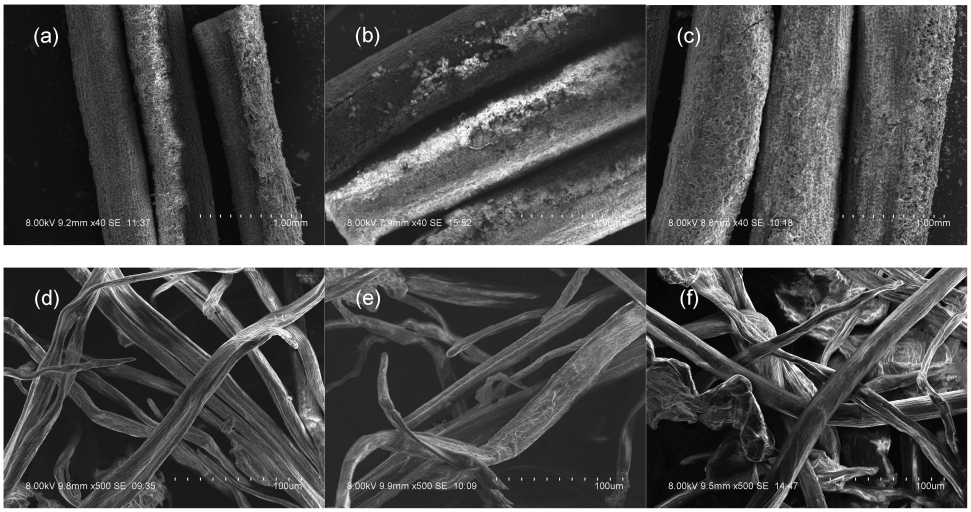

Figure 2: Representative SEM micrographs of OPT fibers at (**a**) 21 years, (**b**) 25 years and (**c**) 32 years (40× magnification) and cellulose extracted from OPT at (**d**) 21 years, (**e**) 25 years and (**f**) 32 years (500× magnification).

Following cellulose extraction, clear morphological changes were observed for all age groups (Fig. 2d–f). The extracted celluloses exhibited more fibrillated and individualized fibers with reduced surface deposits compared to the raw OPT, indicating effective removal of lignin, hemicellulose, and other matrix components during the chemical treatments. At the magnification employed, the overall surface texture and fibrillar morphology of celluloses from OPT aged 21, 25, and 32 years were broadly similar, and no pronounced differences in surface smoothness were evident. However, cellulose from the 32-year-old trunk (Fig. 2f) showed a slightly higher degree of fiber separation, suggesting slightly improved defibrillation and accessibility of the cell wall structure in the more mature material, consistent with reports that more extensive delignification leads to cleaner and more individualized cellulose fibrils [2].

This interpretation is further supported by the cellulose yield obtained after chemical extraction, which increased slightly with trunk age, from 51.16% for OPT21 to 52.33% for OPT25 and 53.41% for OPT32. The higher yield for OPT32 indicates more effective removal of non-cellulosic components during delignification and bleaching, which is consistent with the cleaner and more individualized fibrillar morphology observed in the SEM micrographs, as similarly reported for chemically treated oil palm biomass and other lignocellulosic fibers [17].

The observed morphological differences indicate that palm age significantly influences the quality and structure of cellulose obtained from OPT. Older OPT appears to yield more refined cellulose fibers with improved separation and reduced agglomeration, characteristics that are desirable for renewable material applications such as bio-composites, packaging films, and polymer reinforcements. The enhanced surface area and fiber network in the 32-year-old sample could improve interfacial adhesion with polymer matrices, offering potential for superior mechanical performance and durability [18,19].

3.2 Functional Group Analysis

Fig. 3a presents the FTIR spectra of the extracted celluloses from OPT aged 21, 25, and 32 years, alongside commercial cellulose for comparison. All samples exhibited the characteristic absorption bands of

cellulose, thereby confirming successful isolation of the polysaccharide. The broad absorption band in the region of 3300–3400 cm^{-1} corresponds to the stretching vibrations of the hydroxyl groups (O-H) typical of cellulose and corresponds to its hydrophilicity and moisture interactions. The peak observed near the region of 2900 cm^{-1} is attributed to the stretching of the aliphatic saturated C–H of methylene groups in cellulose [20]. All samples in Fig. 3a showed a prominent absorption band near 1030 cm^{-1}, corresponding to C–O–C stretching of β-glycosidic linkages of the pyranose ring and glycosidic bonds in cellulose. These features are consistent with the spectral profile of cellulose derived from OPT, as previously reported by Mazlita et al. [21].

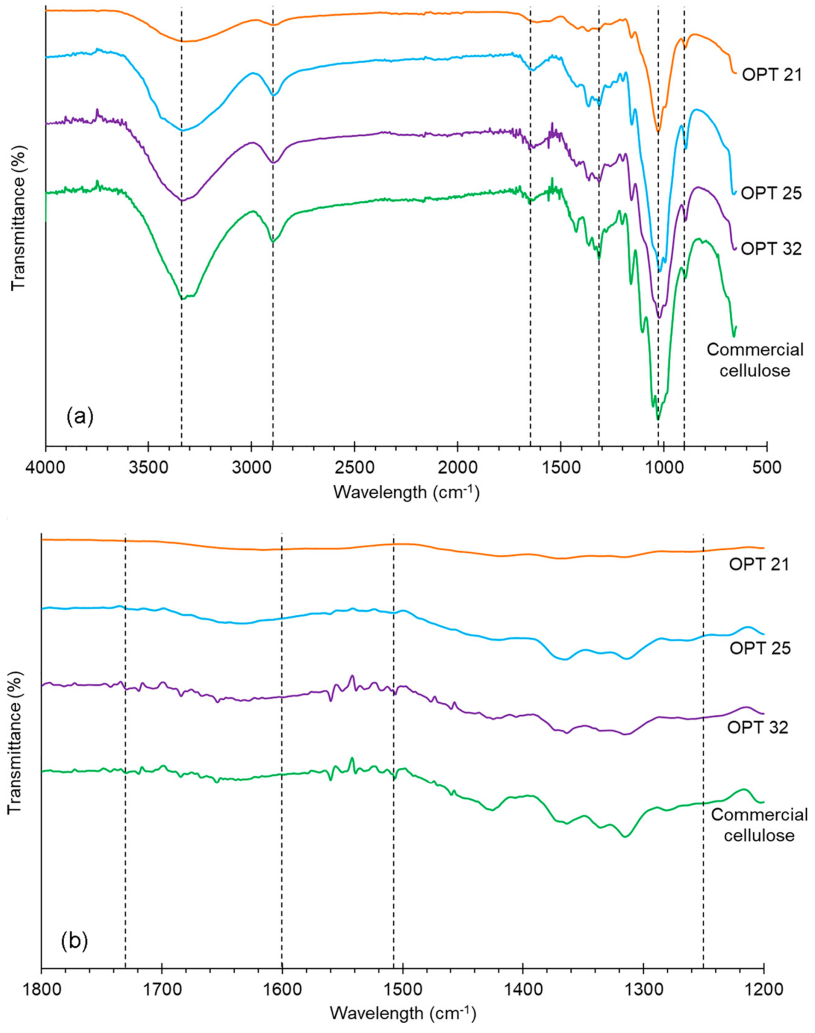

Figure 3: FTIR spectra of cellulose extracted from OPT at 21, 25, and 32 years, compared with commercial cellulose. (**a**) Full spectral range (4000–500 cm^{-1}) and (**b**) enlarged fingerprint region (1800–1200 cm^{-1}) highlighting the absence of non-cellulosic impurities and age-dependent variations in crystalline-sensitive bands.

The small shoulder around 1640 cm^{-1} is associated with absorbed water, representing the bending mode of H–O–H, commonly observed in hydrophilic polysaccharides. The peaks between 1425–1430 cm^{-1} and 1315–1320 cm^{-1} correspond to CH_2 scissoring and C–H bending, respectively, indicating the ordered structure of cellulose. Additionally, the prominent band near 1030–1050 cm^{-1} represents C–O–C stretching of β-1,4-glycosidic linkages, while the sharp peak observed at 897 cm^{-1} is attributed to C_1–H glucose ring

stretching, a defining marker of cellulose chains [6]. The spectra of OPT-derived celluloses closely match that of commercial cellulose, with only minor intensity variations likely related to age-dependent differences in cellulose crystallinity and hydrogen-bonding environments. These results collectively confirm that the extraction process effectively yielded high-purity cellulose across all OPT ages.

To further examine the impact of maturity, the FTIR fingerprint region (1200–1700 cm^{-1}) was analyzed in detail (Fig. 3b). The consistent absence of peaks at 1735 cm^{-1} (C=O stretching in hemicellulose) and 1510 cm^{-1} (C=C aromatic stretching in lignin) across all samples confirms that the cellulose isolation method remains highly effective regardless of OPT age. However, age-dependent differences are evident in the 'crystallinity-sensitive' bands; specifically, the absorption intensities at 1425–1430 cm^{-1} and 1315–1320 cm^{-1} become progressively sharper and more pronounced from 21 to 32 years. This enhancement in spectral definition suggests that as the oil palm matures, the cellulose chains undergo greater structural consolidation and molecular ordering. These results indicate that while the chemical purity of the extracted cellulose is uniform, the 32-year OPT yields a product with a more robust and highly ordered crystalline framework, directly correlating with the increased CrI observed in the subsequent XRD analysis (Section 3.3) and aligning with structural trends reported for mature oil palm biomass [22].

3.3 Crystalline Properties

The XRD patterns of cellulose extracted from OPT at 21, 25, and 32 years (Fig. 4) show noticeable differences from commercial cellulose and deviate from the typical features of pure cellulose I. Although a main diffraction peak is present in the region normally associated with the (200) plane, all OPT samples exhibit a slight shift of this peak toward lower 2θ values. Such shifts are commonly reported for alkali-treated or mercerized cellulose and are associated with lattice swelling, disruption of intermolecular hydrogen bonding, and partial conversion from the parallel-chain cellulose I structure to the antiparallel cellulose II arrangement [23–25].

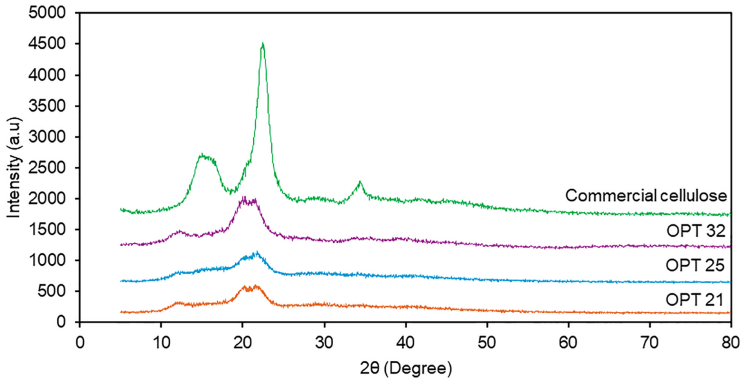

Figure 4: XRD patterns of cellulose from OPT at 21, 25 and 32 years in comparison with commercial cellulose.

In addition, the presence of a single peak near ~12° and a partial splitting of the broad peak in the 20°–23° region resemble the behaviour reported for partially mercerized cellulose, where structural disorder or a mixed cellulose I/II arrangement occurs. These observations suggest that the cellulose isolated from OPT may contain both native cellulose I regions and disordered or cellulose II–like features, rather than a fully preserved cellulose I structure [26]. This structural complexity is consistent with the FTIR findings (Section 3.2), where the sharpening of vibrational bands in mature trunks suggested a higher degree of molecular ordering despite the preservation of a mixed polymorph.

In view of these differences in peak positions, the crystallinity calculation was adjusted by determining the I_{am} value at the amorphous minimum specific to each OPT diffractogram. Using this approach, the CrI of OPT 21, OPT 25, and OPT 32 were calculated as 62.94%, 65.46%, and 68.62%, respectively. Although these CrI values remain lower than that of the commercial cellulose used in this study (83.21%), the increasing trend with tree age remains evident. The increase in crystallinity with palm age can be attributed to structural and compositional changes in the trunk as the palm matures. Older trunks are likely to possess higher cellulose content and lower proportions of amorphous hemicelluloses, leading to enhanced crystalline organisation after extraction [27].

The progressive improvement in CrI from OPT 21 to OPT 32 suggests that cellulose obtained from older palms exhibits greater structural regularity, which could translate into improved performance in structural material applications. This aligns with the intensified 'crystallinity-sensitive' peaks observed in the FTIR fingerprint region (1430 cm^{-1}), confirming that both the chemical bond environment and the crystal lattice become more organized as the biomass matures. From an application standpoint, the higher crystallinity of OPT 32 cellulose implies superior mechanical integrity and thermal stability. Previous studies have demonstrated that cellulose with intermediate crystallinity can serve effectively in composites, films, and other renewable applications where a balance between flexibility and rigidity is needed [25,26]. Therefore, the age-dependent improvement in ordering strongly supports the potential of mature OPT as a sustainable raw material.

3.4 Thermal Properties

The TGA and DTG profiles of cellulose isolated from OPT at 21, 25, and 32 years exhibited the characteristic three-stage mass-loss pattern of lignocellulosic cellulose, as shown in Fig. 5. The initial minor loss below 120°C can be attributed to the evaporation of physically adsorbed moisture, followed by the main decomposition step at ~300°C–380°C, corresponding to the depolymerization of cellulose chains and breakdown of glycosidic linkages. The DTG traces show a single sharp maximum (T_{max}) that systematically shifts upward with increasing trunk age (OPT-21 < OPT-25 < OPT-32), indicating that older trunks yield cellulose with enhanced thermal stability. This trend provides strong evidence that trunk maturity plays a decisive role in tailoring cellulose thermal behavior, where prolonged growth leads to more ordered molecular packing and hence greater resistance to thermal degradation [27]. In comparison, the commercial cellulose standard exhibited a narrower degradation event with a steeper peak, indicating its higher homogeneity and purity [28].

The enhanced thermal resistance of cellulose derived from older oil palm trunks can be associated with its higher crystallinity, as previously confirmed by XRD analysis (Section 3.3). The more ordered crystalline domains restrict the mobility of cellulose chains and increase the energy required for decomposition, thereby delaying the onset of thermal degradation [29]. Such structure–property relationships highlight the synergistic role of cellulose microstructure in dictating its end-use processing stability, which is particularly relevant for polymer reinforcement and high-temperature composite fabrication. This correlation between crystallinity and thermal stability has been well-documented in previous studies on natural fiber celluloses [17,24]. In addition, the relatively higher char residue of OPT cellulose compared to the commercial cellulose suggests the presence of residual non-cellulosic constituents, such as lignin or inorganic minerals, which are known to enhance char formation during pyrolysis [30]. This residual char fraction is advantageous in certain applications, for example, flame-retardant or insulating composites, where char acts as a protective barrier against further degradation. Such behavior is consistent with other agricultural-residue-derived celluloses, which often retain trace amounts of matrix components even after chemical treatment [31,32].

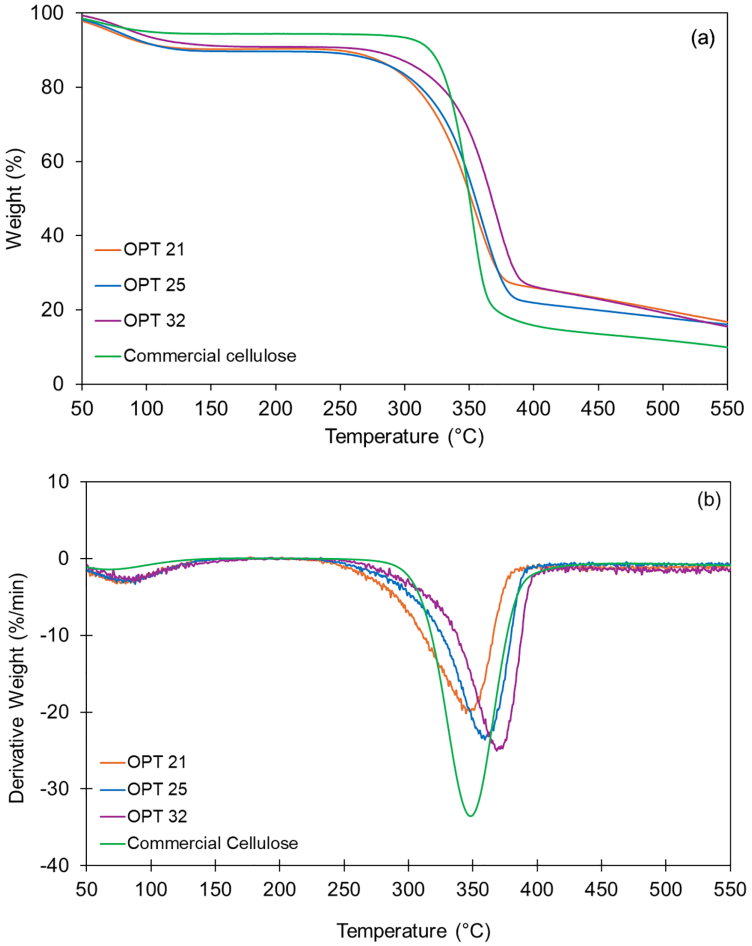

Figure 5: (**a**) TGA and (**b**) DTG curves of cellulose extracted from OPT at 21, 25 and 32 years in comparison with commercial cellulose.

When compared with related oil palm biomass resources, the thermal degradation characteristics of OPT cellulose are in close agreement with earlier reports. Cellulose isolated from OPF displayed maximum degradation peaks in the 330°C–360°C range, with increasing crystallinity leading to improved stability [20]. Similarly, cellulose obtained from oil palm EFB showed a single DTG maximum within 325°C–365°C, with optimized delignification producing more thermally stable cellulose fractions [33]. For OPT-derived nanocellulose, Lamaming et al. [7] reported degradation peaks in the mid-350°C region, corroborating the present findings for OPT samples. In this study, the cellulose obtained from 32-year-old trunks demonstrated the highest thermal stability, aligning with previous literature. This further highlights the suitability of mature OPT cellulose for renewable-material applications that require resistance to thermal stresses encountered during processing.

4 Conclusions

This study demonstrated that the properties of cellulose extracted from OPT are strongly influenced by palm age. Younger trunks yielded cellulose with lower crystallinity and reduced thermal stability, while older trunks produced cellulose with higher crystalline order and greater resistance to thermal degradation. These variations reflect the progressive structural reorganisation of the lignocellulosic matrix during maturation and highlight the critical influence of trunk age on cellulose quality. From an application perspective,

cellulose derived from younger OPT, owing to its relatively higher amorphous content and reactivity, is well-suited for chemical derivatization into value-added products. In contrast, cellulose obtained from older OPT, with its enhanced crystallinity and stability, holds greater potential for reinforcing biocomposites, biodegradable films, and other advanced renewable materials requiring durability. Overall, the findings establish a clear age-performance relationship, providing a scientific basis for selecting OPT of optimal maturity to maximize functional performance and advance the sustainable valorization of this abundant biomass resource.

Acknowledgement: The authors are grateful to the Malaysian Palm Oil Board (MPOB) for providing the financial support for this study and for permission to publish this research paper. Additionally, the authors wish to express their sincere appreciation to the Biomass Technology Unit and the Agronomy and Geospatial Technology Unit of MPOB, and the iCRIM Centralised Laboratory of Universiti Kebangsaan Malaysia for their valuable technical support throughout this study.

Funding Statement: The authors received no specific funding.

Author Contributions: The authors confirm contribution to the paper as follows: Writing—original draft preparation, investigation, formal analysis and data curation, Elina Hishamuddin; writing—review and editing, Humaira Alias Aisyah; data curation and resources, Fatiha Ismail and Stasha Eleanor Rosland Abel; supervision, Abdul Wahab Noorshamsiana. All authors reviewed and approved the final version of the manuscript.

Availability of Data and Materials: The authors confirm that the data supporting the findings of this study are available within the article.

Ethics Approval: Not applicable.

Conflicts of Interest: The authors declare no conflicts of interest.

References

1. Pulingam T, Lakshmanan M, Chuah JA, Surendran A, Zainab-L I, Foroozandeh P, et al. Oil palm trunk waste: environmental impacts and management strategies. Ind Crops Prod. 2022;189:115827. doi:10.1016/j.indcrop.2022.115827.
2. Zaini LH, Gindl-Altmutter W, Gusenbauer C, Rahayu IS, Lubis MAR, Mautner A, et al. Nanofibrils from oil palm trunk: effect of delignification and fibrillation technique. J Wood Sci. 2024;70(1):19. doi:10.1186/s10086-024-02133-5.
3. Zaini LH, Surisetty J, Lammer H, Veigel S, Gindl-Altmutter W. The suitability of fibers from the inner part of oil palm trunks for molded pulp packaging materials. Ind Crops Prod. 2025;234(4):121506. doi:10.1016/j.indcrop.2025.121506.
4. Aisyah HA, Hishamuddin E, Noorshamsiana AW, Ibrahim Z, Ilyas RA. Oil palm fiber hybrid composites: a recent review. J Renew Mater. 2024;12(10):1661–89. doi:10.32604/jrm.2024.055217.
5. Mohammad Taib MNA. Influence of green fillers from oil palm trunk (*Elaeis guineensis*) on the thermal stability, tensile performance and morphological properties of reinforced epoxy composites. RSC Adv. 2025;15(53):45061–70. doi:10.1039/d5ra07482g.
6. Lamaming J, Hashim R, Sulaiman O, Leh CP, Sugimoto T, Nordin NA. Cellulose nanocrystals isolated from oil palm trunk. Carbohydr Polym. 2015;127(2):202–8. doi:10.1016/j.carbpol.2015.03.043.
7. Lamaming J, Chai CHEW S, Hashim R, Sulaiman O, Sugimoto T. Extraction of microcrystalline cellulose from oil palm trunk. J Jpn Inst Energy. 2017;96(11):513–8. doi:10.3775/jie.96.513.
8. Ng LY, Wong TJ, Ng CY, Amelia CKM. A review on cellulose nanocrystals production and characterization methods from *Elaeis guineensis* empty fruit bunches. Arab J Chem. 2021;14(9):103339. doi:10.1016/j.arabjc.2021.103339.

9. Mohd Rasli SRA, Ahmad I, Mat Lazim A, Hamzah A. Extraction and characterization of cellulose from agricultural residue—Oil palm fronds. Malays J Anal Sci. 2017;21(5):1065–73. doi:10.17576/mjas-2017-2105-08.
10. Okahisa Y, Furukawa Y, Ishimoto K, Narita C, Intharapichai K, Ohara H. Comparison of cellulose nanofiber properties produced from different parts of the oil palm tree. Carbohydr Polym. 2018;198:313–9. doi:10.1016/j.carbpol.2018.06.089.
11. Park S, Baker JO, Himmel ME, Parilla PA, Johnson DK. Cellulose crystallinity index: measurement techniques and their impact on interpreting cellulase performance. Biotechnol Biofuels. 2010;3(1):10. doi:10.1186/1754-6834-3-10.
12. TAPPI Standard T 257 cm-22. Sampling and preparing wood for analysis. Atlanta, GA, USA: Technical Association of the Pulp and Paper Industry (TAPPI); 2022.
13. Wise LE, Murphy M, Adieco AAD. A chlorite holocellulose, its fractionation and bearing on summative wood analysis and studies on the hemicelluloses. Nat Environ Pollut Technol. 1946;23(1):427–34. doi:10.1021/ac60007a010.
14. TAPPI Standard T 203 cm-22. Alpha-, beta- and gamma-cellulose in pulp. Atlanta, GA, USA: Technical Association of the Pulp and Paper Industry (TAPPI); 2022.
15. Segal L, Creely JJ, Martin AE Jr, Conrad CM. An empirical method for estimating the degree of crystallinity of native cellulose using the X-ray diffractometer. Text Res J. 1959;29(10):786–94. doi:10.1177/004051755902901003.
16. Noorshamsiana AW. A review on extraction processes of lignocellulosic chemicals from oil palm biomass. J Oil Palm Res. 2018;29(4):512–27. doi:10.21894/jopr.2017.00016.
17. Ajayi SM, Olusanya SO, Didunyemi AE, Abimbade SF, Olumayede EG, Akintayo CO. Physicochemical properties of oil palm biomass waste fibres and its cellulose for engineering applications: a review. Biomass Convers Biorefin. 2025;15(5):6545–55. doi:10.1007/s13399-024-05486-5.
18. Aisyah HA, Azreena IN, Hishamuddin E, Noorshamsiana AW, Nurazzi NM. Enhancements in oil palm fiber for composite material development. J Renew Mater. 2025:1–10. doi:10.32604/jrm.2025.02025-0141.
19. Ramful R. Mechanical performance and durability attributes of biodegradable natural fibre-reinforced composites—A review. J Mater Sci Mater Eng. 2024;19(1):50. doi:10.1186/s40712-024-00198-0.
20. Dungani R, Owolabi AF, Saurabh CK, Abdul Khalil HPS, Tahir PM, Hazwan CICM, et al. Preparation and fundamental characterization of cellulose nanocrystal from oil palm fronds biomass. J Polym Environ. 2017;25(3):692–700. doi:10.1007/s10924-016-0854-8.
21. Mazlita Y, Lee HV, Hamid SBA. Preparation of cellulose nanocrystals bio-polymer from agro-industrial wastes: separation and characterization. Polym Polym Compos. 2016;24(9):719–28. doi:10.1177/096739111602400907.
22. Jonoobi M, Oladi R, Davoudpour Y, Oksman K, Dufresne A, Hamzeh Y, et al. Different preparation methods and properties of nanostructured cellulose from various natural resources and residues: a review. Cellulose. 2015;22(2):935–69. doi:10.1007/s10570-015-0551-0.
23. Mulla MH, Norizan MN, Rawi NFM, Kassim MHM, Abdullah N, Norrrahim MNF. Surface and interfaces effects of concentrations and alkaline treatment durations on sugar palm fiber as structural reinforcement in polymer composites. J Nat Fibres. 2025;22(1):2527277. doi:10.1080/15440478.2025.2527277.
24. Kim S, Hwang K, Lee J, Chun SJ, Lee D, Kim Y, et al. Contribution of structural changes in cellulose fibers induced by alkali treatment to their nanofibrillation. ACS Omega. 2025;10(41):49087–97. doi:10.1021/acsomega.5c07902.
25. Zhang D, Fang Z, Hu S, Qiu X. High aspect ratio cellulose nanofibrils with low crystallinity for strong and tough films. Carbohydr Polym. 2024;346:122630. doi:10.1016/j.carbpol.2024.122630.
26. Fernández-Santos J, Valls C, Cusola O, Roncero MB. Composites of cellulose nanocrystals in combination with either cellulose nanofibril or carboxymethylcellulose as functional packaging films. Int J Biol Macromol. 2022;211:218–29. doi:10.1016/j.ijbiomac.2022.05.049.
27. Korom A, Phua MH, Matsuura T. Relationships between crown size and aboveground biomass of oil palms: an evaluation of allometric models. Sains Malays. 2016;45:523–33.
28. Mohamad Haafiz MK, Hassan A, Zakaria Z, Inuwa IM. Isolation and characterization of cellulose nanowhiskers from oil palm biomass microcrystalline cellulose. Carbohydr Polym. 2014;103(2):119–25. doi:10.1016/j.carbpol.2013.11.055.

29. Abdul Khalil HPS, Bhat AH, Ireana Yusra AF. Green composites from sustainable cellulose nanofibrils: a review. Carbohydr Polym. 2012;87(2):963–79. doi:10.1016/j.carbpol.2011.08.078.
30. D'Acierno F, Michal CA, MacLachlan MJ. Thermal stability of cellulose nanomaterials. Chem Rev. 2023;123(11):7295–325. doi:10.1021/acs.chemrev.2c00816.
31. Ionita D, Cristea M, Cosmulescu SF, Predeanu G, Harabagiu V, Samoila P. Thermal and viscoelastic responses of selected lignocellulosic wastes: similarities and differences. Polymers. 2023;15(9):2100. doi:10.3390/polym15092100.
32. Yang H, Yan R, Chen H, Lee DH, Zheng C. Characteristics of hemicellulose, cellulose and lignin pyrolysis. Fuel. 2007;86(12–13):1781–8. doi:10.1016/j.fuel.2006.12.013.
33. Ismail F, Ali Othman NE, Abdul Wahab N, Abdul Hamid F, Abdul Aziz A. Preparation of microcrystalline cellulose from oil palm empty fruit bunch fibre using steam-assisted acid hydrolysis. J Adv Res Fluid Mech Therm Sci. 2021;81(1):88–98. doi:10.37934/arfmts.81.1.8898.